

# Native *E. coli* inner membrane incorporation in solid-supported lipid bilayer membranes

Charlotte E. Dodd, Benjamin R. G. Johnson, and Lars J. C. Jeuken  
*School of Physics and Astronomy, University of Leeds, Leeds, LS2 9JT, United Kingdom*

Timothy D. H. Bugg  
*Department of Chemistry, University of Warwick, Coventry, CV4 7AL, United Kingdom*

Richard J. Bushby  
*Centre for Self-Organising Molecular Systems, University of Leeds, Leeds, LS2 9JT, United Kingdom*

Stephen D. Evans<sup>a)</sup>  
*School of Physics and Astronomy, University of Leeds, Leeds, LS2 9JT, United Kingdom*

(Received 26 November 2007; accepted 21 February 2008; published 30 April 2008)

Solid-supported bilayer lipid membranes (SBLMs) containing membrane protein have been generated through a simple lipid dilution technique. SBLM formation from mixtures of native *Escherichia coli* bacterial inner membrane (IM) vesicles diluted with egg phosphatidylcholine (egg PC) vesicles has been explored with dissipation enhanced quartz crystal microbalance (QCM-D), atomic force microscopy (AFM), attenuated total internal-reflection Fourier-transform infrared spectroscopy (ATR-FTIR), and fluorescence recovery after photobleaching (FRAP). QCM-D studies reveal that SBLM formation from vesicle mixtures ranging between 0% and 100% IM can be divided into two regimes. Samples with  $\leq 40\%$  IM form SBLMs, while samples of greater IM fractions are dominated by vesicle adsorption. FRAP experiments showed that the bilayers formed from mixed vesicles with  $\leq 40\%$  IM were fluid, and comprised a mixture of both egg PC and IM. ATR-FTIR measurements on SBLMs membranes formed with 30% IM confirm that protein is present. SBLM formation was also explored as a function of temperature by QCM-D and FRAP. For samples of 30% IM, QCM-D data show a decreased mass and viscoelasticity at elevated temperatures, and an increased fluidity is observed by FRAP measurements. These results suggest improved biomimetic characteristics can be obtained by forming and maintaining the system at, or close to, 37 °C. © 2008 American Vacuum Society. [DOI: 10.1116/1.2896113]

## I. INTRODUCTION

Cellular organisms are ubiquitous and without exception contain lipid membrane structures as barriers at the exterior cell perimeter and, for eukaryotes, to create subcompartments within cells. Communication between cells and their surroundings is mediated in a variety of ways, often through membrane proteins, which also play a role in processes such as endocytosis.<sup>1</sup> Membrane proteins account for a large fraction of all proteins—approximately 20–30% of the human genome encodes for membrane proteins.<sup>2–5</sup> They also mediate processes such as energy transfer,<sup>6</sup> light harvesting,<sup>7</sup> and cell division.<sup>8</sup> They have also been implicated in diseases such as asthma,<sup>9</sup> cancer,<sup>10</sup> and Alzheimer's,<sup>11,12</sup> and as a result they account for approximately two thirds of all protein drug targets.<sup>4,13</sup>

The study of membrane proteins or the processes which they mediate is an extremely difficult task in whole cells due to their enormous complexity. As a consequence of this, there is a wide interest in the development of “artificial” membrane systems, in the form of vesicles, lipid monolayers, and solid-supported lipid bilayers. Solid-supported bilayer lipid membranes (SBLMs) can be generated in a variety of

ways. In the most simple approach, SBLMs are formed by the adsorption and rupture of vesicles onto various different substrates, as pioneered by McConnell some 20 years ago.<sup>14,15</sup> Tethered bilayer lipid membranes (TBLMs) are fabricated in a similar fashion, but rather than being formed on unmodified SiO<sub>2</sub> or mica supports, a self-assembled monolayer is used to anchor the bilayer to the surface.<sup>16,17</sup> The formation of SBLMs/TBLMs provides the opportunity to employ a wide range of surface analytical techniques, such as atomic force microscopy (AFM),<sup>18,19</sup> dissipation enhanced quartz crystal microbalance (QCM-D),<sup>20,21</sup> surface plasmon resonance (SPR),<sup>22–24</sup> fluorescence recovery after photobleaching (FRAP),<sup>25</sup> or attenuated total internal-reflection Fourier-transform infrared (ATR-FTIR) spectroscopy,<sup>26,27</sup> all of which can yield complementary information about the system under study.

To date, several approaches have been used to facilitate protein incorporation into SBLMs. In general, proteins are either purified and reconstituted into lipid vesicles, which are then used to form SBLMs,<sup>19</sup> or alternatively, lipid bilayers are formed and then are incubated with the desired proteins.<sup>28,29</sup> Incorporating proteins in these ways is effective when only relatively small amounts of a single protein are needed. However, as the number of proteins required for an active system increases, the process becomes more complex.

<sup>a)</sup>Author to whom correspondence should be addressed; electronic mail: s.d.evans@leeds.ac.uk

An alternative route is through isolation of the entire cell membrane, production of vesicles from this, and their employment in generating a lipid membrane.<sup>30</sup> However, most cellular membranes are composed largely of protein (for example, bacterial membranes consist of as much as 50–60% protein<sup>31,32</sup>), which poses a problem when attempting to form a SBLM. A recent study by Graneli *et al.*<sup>33</sup> detailing bilayer formation with proteoliposomes highlighted that extramembranous domains of membrane proteins hinder vesicle rupture. In addition to the difficulties in forming SBLMs from vesicles of such high protein content, the lipid composition of the chosen cellular membrane may also disfavor bilayer formation, for example, the phospholipids found in *E. coli* inner membrane are predominantly unsaturated phosphatidylethanolamine and phosphatidylglycerol.<sup>34,35</sup>

Here, we have explored the formation of solid-supported bilayer membranes using a mixture of *E. coli* inner membrane vesicles (IM) diluted with egg phosphatidylcholine vesicles (egg PC), a lipid which is well characterized and readily forms a solid-supported planar bilayer on glass/silicon (SiO<sub>2</sub>) substrates. Our approach is similar to the method first used by Schneider *et al.* in 1980, who investigated electron transfer mechanisms,<sup>36</sup> in which phospholipid vesicles were generated through sonication, mixed with the inner membrane of mitochondria; fusion was achieved through careful adjustments of the pH. This method was recently adapted by Elie-Caille *et al.*,<sup>37</sup> who were also using a mitochondrial inner membrane in order to study the electron transfer machinery on solid-supported lipid membranes. In this case the sonicated phospholipid vesicles were partially biotinylated and, after mixing with the mitochondrial membranes, the two were sonicated together to promote fusion. The solid supports were functionalized with streptavidin before incubating with the biotinylated proteoliposomes. Fusion was then triggered by the addition of a polyethyleneglycol-containing solution to generate planar membranes.

Our strategy here has been to use separately tip sonicated egg PC vesicles mixed with tip sonicated *E. coli* inner membrane vesicles, which fuse on to a SiO<sub>2</sub> substrate, to form a SBLM. This approach has allowed us to generate SBLMs with a range of naturally occurring bacterial membrane proteins, and thereby allows us to study various bacterial membrane processes as well as interactions with biologically relevant molecules such as antimicrobial peptides. Of particular interest to us is to generate a minimal system that permits the *in vitro* biosynthesis of peptidoglycan, a structural component of the bacterial cell wall.<sup>30</sup>

## II. MATERIALS AND METHODS

### A. Materials

Ultrapure Milli Q (Millipore) water of 18.2 MΩ was used for all cleaning procedures, sample preparation, and buffers. The buffer used in all experiments referred to in this text was Tris-HCl (20 mM, pH 7.4, Melford Laboratories, UK) and the fluorophores used in the FRAP experiments

were Texas Red (DHPE Texas Red) and NBD (nitrobenzoxadiazole (C6-HPC)), both Molecular Probes, Invitrogen (Eugene, OR). Sodium dodecyl sulfate (SDS) used for cleaning was diluted to 0.4% (w/v) (Sigma Aldrich, Dorset, UK). Decon 90 (Hove, UK) used for ATR prism and glass cleaning was diluted to 2% (v/v), chloroform, propan-2-ol, and methanol used was from Fisher (HPLC grade, Loughborough, UK). For “piranha” cleaning, hydrogen peroxide and sulfuric acid were purchased from Sigma Aldrich (Dorset, UK). Other materials used include pre-cut silicon substrates for AFM experiments (5×5 mm, Agar Scientific, Essex, UK), glass coverslip for FRAP experiments (Menzel GmbH, Braunschweig, Germany), and silicon dioxide sensor crystals (5 MHz) for the QCM-D experiments (Q-Sense AB, Gothenburg, Sweden). L- $\alpha$ -phosphatidylcholine (egg PC) lipid used in this work was purchased from Avanti Polar Lipids (Alabaster, AL).

### B. Isolation of *E. coli* inner membrane

*E. coli* [strain BL21(DE3)] were grown overnight at 37 °C in 2YT media (16 g/L Tryptone, 10 g/L yeast extract, 5 g/L NaCl, pH 7.5) and harvested by centrifugation. The cells were then washed several times in buffer (20 mM Tris-HCl pH 7.5), finishing in a minimum volume of buffer. The cells were disrupted using a cell disruptor (Constant Systems Ltd, Daventry, UK),<sup>38</sup> after which the solution was centrifuged at 12 000 g for 1 h to remove cellular debris. High speed centrifugation (131 000 g) was used to sediment the vesicles; these were subsequently solubilized in Tris-EDTA buffer (20 mM Tris-HCl, 0.5 mM EDTA, pH 7.5). A sucrose gradient was used to separate the inner from the outer membrane vesicles. The inner membrane vesicles were collected from the sucrose gradient and washed several times with Tris-EDTA buffer to remove the sucrose. The protein concentration was determined using a BCA assay<sup>39</sup> and the vesicle solution stored at –80 °C until use.

### C. Sample preparation

Egg PC lipid was dissolved in a 1:1 solution of chloroform:methanol and divided into aliquots. These were then dried under nitrogen for 20 min, and desiccated for not less than 1 hour. Aliquots were stored under nitrogen at –20 °C prior to use. Vesicle solutions of egg PC were prepared by resuspension of the lipids in buffer (5 mg/ml) with vortexing, and then tip sonicated at 4 °C until the solution no longer appeared cloudy (ca. 30 min for 1 ml). The solution was then centrifuged for 1 min at 14 500 g to remove titanium particles. Vesicle solutions of the *E. coli* inner membrane, produced as described earlier, were diluted to 2.5 mg/ml in buffer while vortexing to aid thawing. These suspensions were then tip sonicated for 20 min until the solution no longer appeared cloudy, following which the solution was centrifuged for 1 min at 14 500 g. Egg PC tip sonicated vesicles, measured by transmission electron microscopy, were typically 20–30 nm diameter, while IM tip sonicated vesicles were typically within the range 50–100

nm. The two vesicle preparations (egg PC and IM) were mixed together in the required ratios and diluted to 0.5 mg/ml before use. Samples were used within 2 days of preparation.

#### D. Substrate cleaning

Silicon wafers for AFM and silicon dioxide coated QCM-D sensor crystals were both cleaned by sonication for 15 min in 0.4% (w/v) SDS followed by thorough rinsing in ultrapure water, before a further 15 min sonication and thorough rinsing in ultrapure water, and finally dried under oxygen-free nitrogen. The substrates were then further treated for 30 min with UV/ozone (UV/ozone cleaning system, low pressure quartz-mercury vapor lamp emitting 254 and 185 nm UV, UVOCS, Montgomeryville) followed by rinsing in ultrapure water, and dried under oxygen-free nitrogen. Glass coverslips for the FRAP experiments were cleaned through sonication in Decon 90 (2%) for 15 min, rinsed and sonicated for 15 min in ultrapure water, rinsed and sonicated in methanol for 15 min, and finally dried with oxygen-free nitrogen. This was followed by immersion for 5 min in "piranha" solution (30:70 hydrogen peroxide:sulfuric acid) (caution: piranha solution reacts violently with many organic materials and should be handled with extreme care), before extensive rinsing and 15 min sonication with ultrapure water. Silicon ATR prisms were cleaned by immersion in 10% Decon 90 for 1 h, followed by extensive rinsing in ultrapure water. The crystals were then immersed for a further hour in methanol and dried with oxygen-free nitrogen. Crystals were subsequently exposed for 30 min to UV/ozone, rinsed in ultrapure water, then propan-2-ol, and dried with oxygen-free nitrogen. In all cases surfaces were cleaned immediately prior to use.

#### E. Atomic force microscopy

AFM measurements were made on silicon substrates. These were incubated with the vesicle mixtures for 1 h, followed by rinsing in buffer. Samples were imaged using a Multimode AFM on a Nanoscope III with an E scanner (Digital Instruments, Veeco Metrology Group, Inc., CA) controller and using Veeco oxide sharpened silicon nitride cantilevers, with a spring constant of approximately 0.06 N/m. Cantilevers were exposed to UV/ozone for 20 min prior to use. Images shown here are height images obtained using the tapping (dynamic) mode under buffer at a frequency of approximately 7–9 kHz.

#### F. Quartz crystal microbalance with dissipation monitoring

QCM-D experiments were performed on the Q-Sense E4 (Q-Sense AB, Gothenburg, Sweden).<sup>21,40</sup> Experiments were performed using silicon dioxide sensor crystals at 22.0 °C, and with the flow held at 40  $\mu$ L/min. Changes in the dissipation,  $D$ , and normalized frequency,  $f$  ( $f = f_n/n$ , where  $n$  is the number of the overtone, i.e.,  $n = 3, 5, 7$ , etc.) of the fifth overtone ( $n = 5$ , 25 MHz) are presented in this work. Vesicles

and buffer used were degassed under vacuum and incubated at the appropriate temperature in a block heater (Grant Instruments, Cambridge) before being introduced to the system.

#### G. Fluorescence recovery after photobleaching

Egg PC was tagged with 1% DHPE Texas Red fluorophore (lipid-bound, head group fluorophore). Samples of IM were tagged by adding 3% C6-HPC NBD (in methanol) (lipid-bound, tail group fluorophore) directly to the inner membrane vesicle extract. The vesicle suspension was then centrifuged (100 000 g for 1 h) to remove any nonvesicle incorporated fluorophore. The fluorophore tagged lipids (both egg PC and IM) were tip sonicated into vesicles separately, as described above, and mixed into the desired ratios before incubation. Freshly cleaned glass coverslips were then incubated with the vesicle suspensions for a period of 30 min. After this time, the sample was rinsed thoroughly with buffer. FRAP experiments were carried out by epifluorescence, using a circular aperture of 30  $\mu$ m diameter and a bleach time of 15 s. The recovery was monitored at regular intervals until the maximum recovery had occurred [Nikon, Eclipse E600 microscope, Hamamatsu Orca ER camera, Data acquisition: Image Pro Express (Media Cybernetics), Image processing: IMAGEJ (freeware)]. For temperature-dependent experiments samples were heated with a custom-built Peltier controller.

From the images obtained, the intensity of a reference area and the photobleach area was measured and used to normalize the photobleach area intensity, to correct for intrinsic photobleaching arising from image acquisition. The background intensity normalized change,  $I_t$  (Figs. 3 and 8) was obtained using the equation  $I_t = i_{b_t} + (i_{r_0} - i_{r_t})$ , where  $i_{b_t}$  was the photobleach area intensity at time  $t$ ,  $i_{r_0}$  the reference area intensity immediately after photobleaching, and  $i_{r_t}$  the reference area intensity at time  $t$ .

The area used for calculation of the diffusion coefficient ( $D$ ) was taken from a Gaussian profile of the bleached region immediately after photobleaching. This accounts for the "corona" effect due to diffusion of the fluorophore during the photobleach period. The recovery was fitted using a Box-Lucas fit to calculate the  $t_{1/2}$  (half-life of recovery), which was then used in the equation  $D = 0.224r^2/t_{1/2}$  to calculate the diffusion coefficient.<sup>25,41</sup> The ideal method for fitting the recovery and calculating  $D$  uses modified Bessel functions and is relatively complex.<sup>25,41,42</sup> A simplified approximation to this fit uses an exponential function, which returns a slightly lower value for  $D$ .<sup>42</sup> For interpretation of the work presented here, however, the more complex fitting function is not justified.

#### H. ATR-FTIR

ATR-FTIR spectra were measured with a Bruker IFS-66 v/S FTIR spectrometer (Bruker, Ettlingen, Germany). A variable angle unit was used for the experiments (Specac, Orpington, UK). Spectra for both buffer and sample were ob-

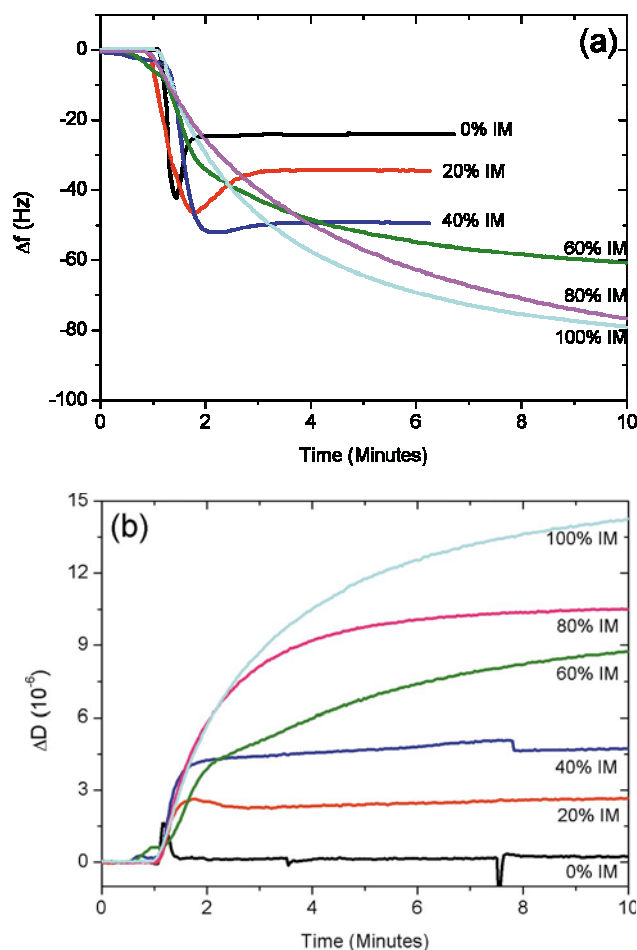


FIG. 1. Change in frequency with time for samples (a) and dissipation (b). Traces are marked as 0% (black), 20% IM (red), 40% IM (blue), 60% IM (green), 80% IM (pink), and 100% IM (turquoise). The pure egg PC bilayer (0% IM) formation has a characteristic shape relating to vesicle adsorption, followed by rupture and loss of encapsulated fluid. Similar behavior is seen for samples of 20 and 40%, in contrast to 60, 80, and 100% in which vesicle adsorption is dominant.

tained using an average of 250 scans at a resolution of  $4 \text{ cm}^{-1}$ . The interferograms measured were zero-filled with two levels, apodized with a Blackman-Harris 3-term function, and Fourier transformed. Spectra are presented in the form of a ratio of  $-1 \text{ g}$  (sample/buffer) to produce an ATR spectrum. The spectra were recorded using  $p$ -polarization illumination and a MCT detector.

### III. RESULTS

A combination of surface analytical techniques has been used to explore the formation of SBLMs, on silicon dioxide surfaces, from solutions containing egg PC and *E. coli* inner membrane vesicles. QCM-D provides information regarding the adsorption kinetics and relative mass uptake, and additionally, the dissipation reveals intermediate stages of vesicle adsorption.<sup>20</sup> AFM yields topological information regarding the adsorbed layers, and FRAP, with multiple fluorophores, gives the fluidity and mobile fraction of different membrane components. Finally, ATR-FTIR is used to confirm the pres-

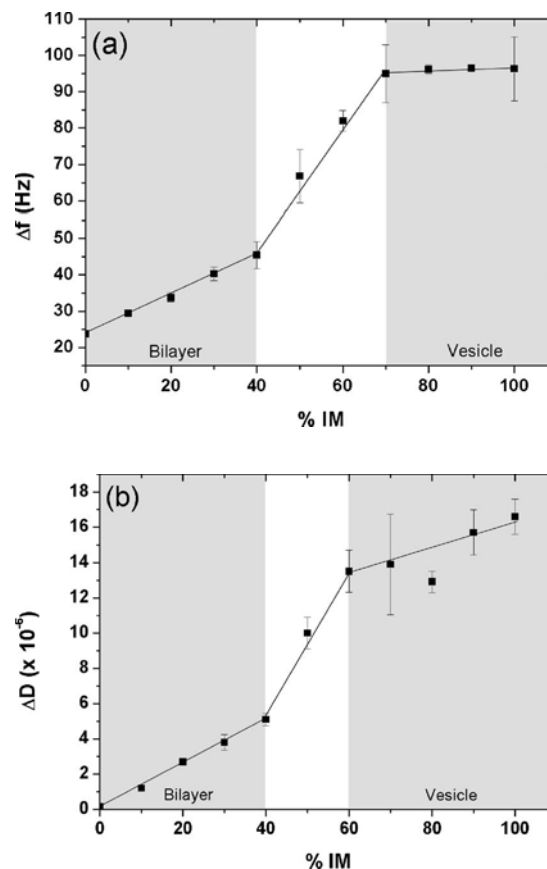


FIG. 2. Plot of the final  $\Delta f$  (a) and  $\Delta D$  (b) vs % IM revealing two distinct regimes. Lines shown are a guide for the eye only and points represent an average of at least three experiments.

ence of protein in the low IM fraction samples.

QCM-D experiments were carried out on samples whose compositions varied between 0% IM (i.e., pure egg PC) and 100% IM in 10% (w/w) increments. Figure 1 shows the variation of frequency as a function of time for a selection of vesicle compositions between 0 and 100% in 20% steps. Typical adsorption kinetics of SBLM formation for the 0% IM (pure egg PC) can be seen in the black traces. Such behavior has been reported previously and is ascribed to vesicle adsorption and rupture.<sup>20</sup> Samples with 10–40% IM retain some of the characteristic behavior associated with rupture of vesicles and the transition to a planar bilayer. The situation is distinctly different in the case of 60–100% IM mixtures, which show no indication of vesicle rupture or SBLM formation, but rather are dominated by Langmuir-type adsorption. When the changes in frequency and dissipation are plotted versus the percent IM content of the vesicle mixtures, two distinct regimes are clearly revealed (Fig. 2). The samples of low IM content display a linear relationship between  $\Delta f$  and  $\Delta D$  signals as a function of IM concentration. Between 40% and 60–70% IM there is a clear jump, beyond which there is little change in  $\Delta f$  or  $\Delta D$ . Although QCM-D data clearly indicate that below 40% IM the surface contains certain SBLM-like features, it does not unambiguously show that the IM vesicles also become part of the SBLM.



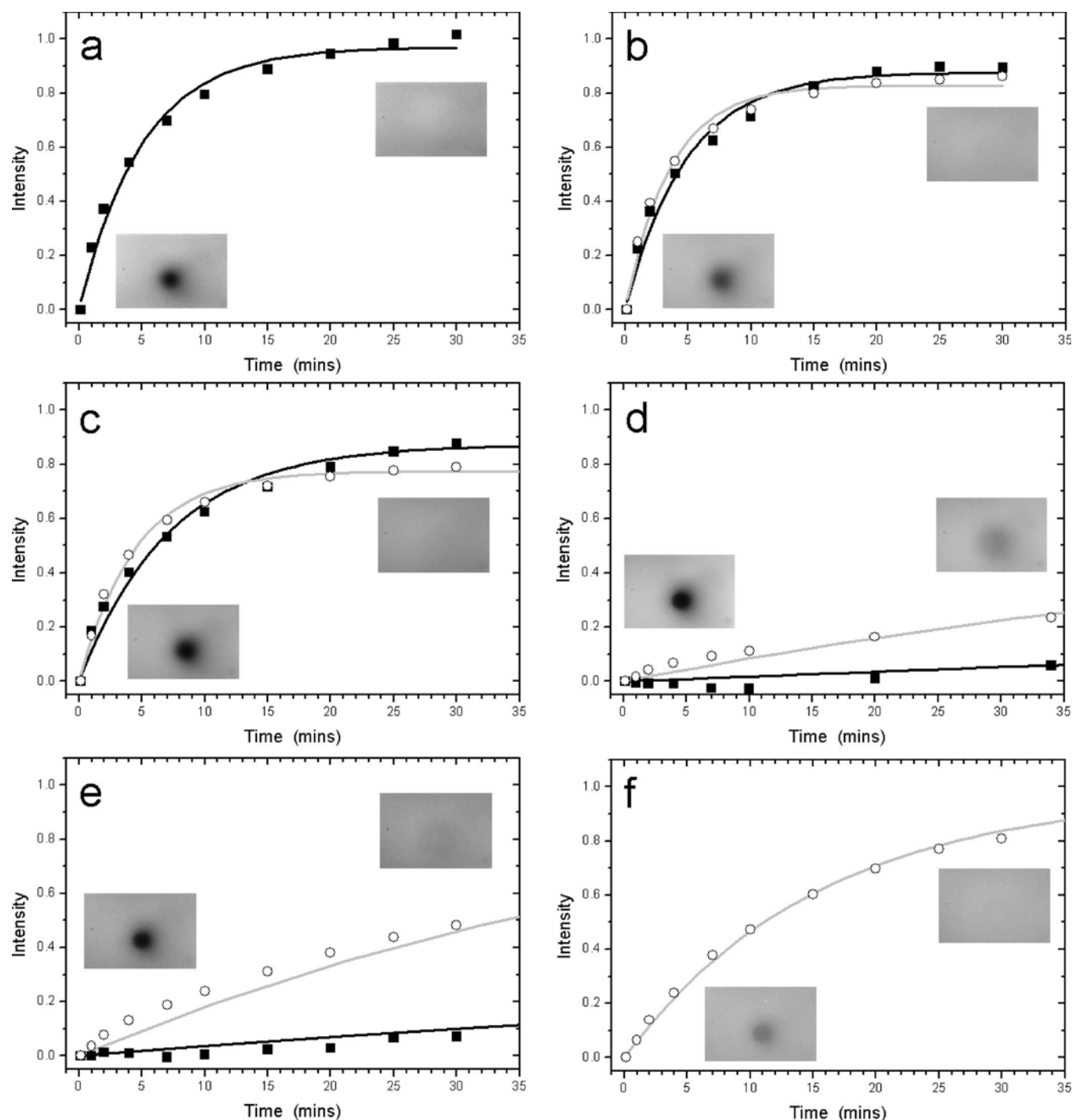


FIG. 3. FRAP data from a range of mixtures of egg PC (tagged with Texas Red marked with black squares) and IM vesicles (tagged with NBD marked with black circles). (a) 0% IM; (b) 20% IM; (c) 40% IM; (d) 60% IM; (e) 80% IM; and (f) 100% IM.

In fluorescence recovery after photobleaching experiments, different fluorophores, Texas Red and NBD, were used to label egg PC [1% (w/w)] and IM (3% (w/w)) vesicles, respectively, prior to mixing. These mixtures were then incubated with glass substrates for 30 min, following which the excess vesicles were flushed away by rinsing with buffer. Figure 3 shows typical recovery curves for both fluorophores as a function of vesicle composition, confirming that both egg PC and IM vesicles contribute to the SBLM

formed. While vesicular mobility could have an influence on the measured diffusion, AFM studies show that there are very few adsorbed vesicles in samples of less than 40% IM, so any influence on the diffusion coefficient is likely to be minimal on samples of less than 40% IM. For IM vesicle concentrations, above the transition, vesicle mobility appears to occur, but at reduced rates in comparison to supported lipid bilayer diffusion coefficients. Samples with 0–40% IM show a rapid recovery of both the NBD and Texas Red fluo-

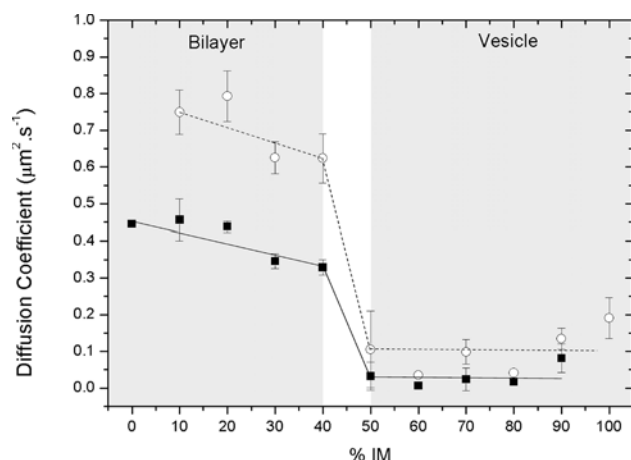


FIG. 4. Diffusion coefficients for the Texas Red tagged egg PC lipids and the NBD tagged IM. Lines shown are an aid for the eye. Each data point is a summary of at least two experiments.

rophores, whereas samples with higher IM content display distinctly different behavior, in which recovery is slow and incomplete.

Intriguingly, the IM vesicles at 80 and 100% appear to show recovery over long time scales (for 80% IM  $t_{1/2}$ =35 min, and for 100% IM  $t_{1/2}$ =10 min) in the FRAP experiments, in spite of evidence from QCM-D that no SBLM is formed. This suggests that IM vesicles adsorbed on the surface retain a certain degree of mobility, unlike the egg PC vesicles labeled with Texas Red. A summary of the diffusion coefficients for the two fluorophores versus IM concentration is presented in Fig. 4. The calculated diffusion coefficients are reduced from typical published values,<sup>42–44</sup> which we believe is due to the corona effect,<sup>45</sup> caused by the long bleach times associated with the use of epifluorescence microscopy. An attempt to take this corona effect into account was made by calculating the diffusion coefficient by fitting a line profile through the middle of the photobleach area with a Gaussian distribution for each of the images, then using the change in Gaussian profile to calculate a value for  $D$ . This method yields a value typically 25% (for a fully mobile system) higher than the values calculated here. It is evident from Fig. 4 that two distinct regimes exist as for the QCM-D data (Fig. 2). Further, we note that the diffusion coefficient appears to be greater for NBD-lipids than for Texas Red. Separate experiments, in which both dyes are used to form SBLMs with egg PC vesicles only, confirm that the difference in diffusion coefficient is due to the nature of the fluorophores—Texas Red lipids are tagged at the head group while NBD is located in the tail group.

AFM was used to image the SBLMs formed as a function of IM concentration; for clarity a subset of these is presented in Fig. 5. Samples with 20% IM show images which are predominantly the same as those of pure egg PC bilayers. Samples with greater than 40% IM show features that are indicative of large numbers of adsorbed vesicles. The presence of SBLMs at lower concentrations was confirmed through force-distance curves (not presented). Cross-

sectional analysis revealed that the larger features seen in the images have sizes concurrent with typical dimensions of adsorbed, flattened vesicles (tip sonicated vesicle size was confirmed through transmission electron microscopy). Examples of these height features can be seen in Fig. 5(f), in which the height protruding above the bilayer is approximately 9 nm. Figure 5(g) shows a cross section taken from the 100% IM membrane shown in Fig. 5(d) clearly showing two vesicles approximately 25 nm in height. A distinctly different regime of smaller features can also be seen in the mixed vesicle samples, with features protruding only a few nanometers from the bilayer, and in some cases less than 1 nm [Fig. 5(b)]. A cross section of these features is shown in Fig. 5(e). Below 40% IM only these smaller features are predominantly observed, which are too small to be adsorbed vesicles.

Although the QCM-D and FRAP indicate that SBLMs are formed when  $\leq 40\%$  IM is used, the possibility exists that little or no proteins from the IM vesicles are transferred to the SBLM. To confirm the presence of protein, ATR-FTIR spectra of SBLMs produced with 30% IM vesicles were recorded (Fig. 6). The amide I and II bands are readily identified in the 30% IM SBLM spectrum, but not in that of the pure egg PC SBLM. In both the egg PC and 30% IM samples a negative band occurs in spectra from 1700–1570  $\text{cm}^{-1}$ , which arises due to water displacement as membranes adsorb on the surface. The band appears negative as the spectra have been in a ratio against the pure buffer spectrum (no displacement), and the difference between the two spectra represents the amount of buffer displaced. This negative contribution also affects the observed amide I absorption in the 30% IM sample, and hence the ratio of the amide I and II bands.

#### A. Effect of temperature on membrane formation

QCM-D was used to follow the formation of SBLMs from samples of 30% IM at different temperatures (22, 25, 30, and 35 °C) by QCM-D. Figure 7 shows the effect of increasing temperature on  $\Delta f$  and  $\Delta D$ . In general, it is seen that the  $\Delta f$  and  $\Delta D$  values move closer to those expected for a pure egg PC lipid bilayer with increasing temperature. In order to corroborate the fact that samples of 30% IM formed at 35 °C comprised fewer vesicles and were more fluid than those formed at 22 °C (as measured with QCM-D in Fig. 7), FRAP experiments were performed, again employing two fluorophores. Figure 8 shows the recovery of both fluorophores in the SBLMs formed with samples of 30% IM at 35 °C; a summary of the resulting diffusion coefficients is given in Table I. A threefold increase in diffusion coefficient was found for Texas Red and a sixfold increase for NBD was found at 35 °C for both fluorophores, which may be due in part to increased thermal diffusion, but may also be indicative of the presence of fewer defects, i.e., protein pinning, incomplete bilayer, or adsorbed vesicles, in the SBLMs formed.

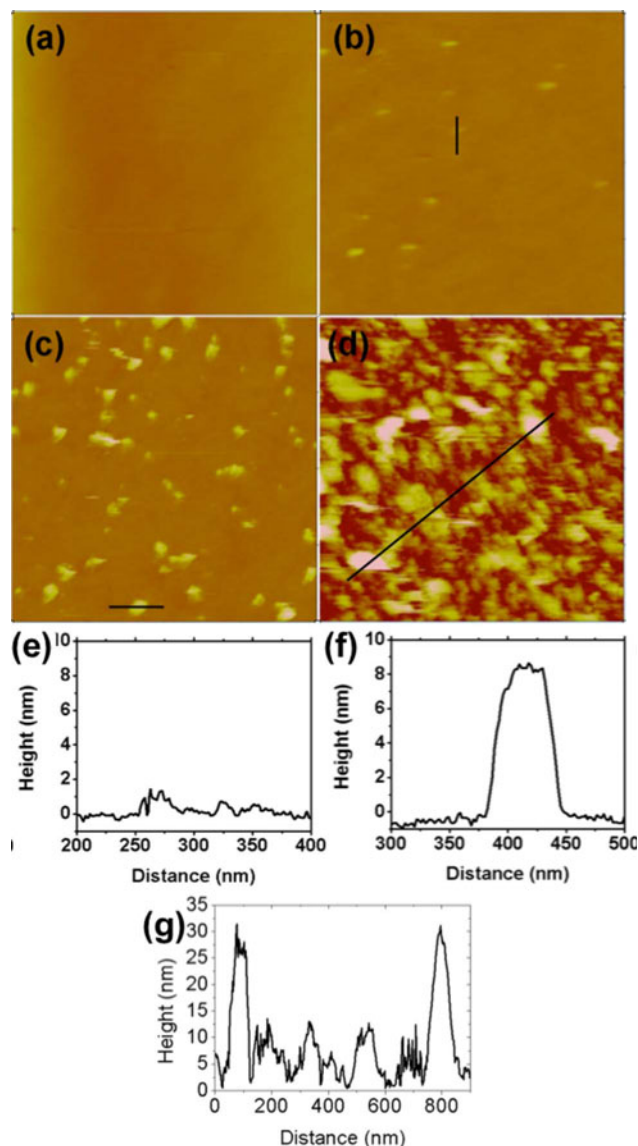


Fig. 5. Tapping mode AFM images of (a) pure egg PC; (b) 20% IM; (c) 50% IM; and (d) 100% IM. (e) is a cross section from image (b), represented by the black line; (f) is a cross section from part of image (c); and (g) is a cross section from image (d). Again, the positions are represented by the black lines. All images presented are on a 1  $\mu\text{m}$  square ( $x,y$ ) and the  $z$  scales are all 30 nm.

#### IV. DISCUSSION

QCM-D allows both bilayer formation or vesicular adsorption to be followed. Figure 1, 0% IM, shows that egg PC lipid vesicles spontaneously form a SBLM, while with 100% IM vesicles the high protein content hampers vesicle rupture and results in an adsorbed vesicle layer. From QCM-D alone, however, it is not possible to determine in detail to what extent SBLMs are formed and to what extent vesicles adsorb intact on the surface. This is particularly true for samples with >50% IM, for which the signal due to vesicle adsorption will mask the comparatively low signal arising from bilayer formation. The change in frequency or dissipation signals represent an average over the whole crystal surface. Therefore, it is not possible to discriminate between signals

from small areas of SBLM with many adsorbed vesicles [i.e., in samples of 60, 80, and 100% IM (Fig. 1)] or occasional adsorbed vesicles in predominantly continuous SBLM [in 20 and 40% IM (Fig. 1)]. AFM, on the other hand, allows SBLM, vesicles and membrane proteins to be distinguished, as can be seen in Figs. 5(a)–5(d). The AFM images of the different IM mixtures confirmed that at high IM ratios the surface is composed predominantly of adsorbed vesicles with small areas of bilayer. In contrast, SBLMs formed with lower fractions of IM contain only a few adsorbed vesicles. The height images shown in Fig. 5 appear to have two classes of features protruding from the bilayer. The highest features, typically around 10–20 nm, are consistent with adsorbed, flattened vesicles; however, the smaller features, less than 2 nm, are below the size range of vesicles. It is possible that these features are due to the incorporation of membrane protein from the inner membrane vesicles. Further, support for the incorporation of membrane protein comes from the observation of the absorption of the amide I and II bands, in ATR-FTIR studies of SBLMs formed with samples of 30% IM. These bands (Fig. 6) are not present in pure egg PC lipid samples, and therefore are present due to the bacterial IM content.

Since tip sonicated egg PC vesicles readily form SBLMs, and bacterial IM vesicles preferentially adsorb intact on the surface, it should be noted that a mixture of the two could lead to formation of a continuous, pure egg PC bilayer with additional adsorbed IM vesicles. Therefore, it is important to note that FRAP studies using two different fluorophores in the egg PC and IM vesicles, presented here in Fig. 3, indicate that both egg PC and IM vesicles rupture and form a single, continuous SBLM with minimum vesicle adsorption occurring in low IM fraction mixtures. Since solutions of pure IM vesicles, in the absence of egg PC vesicles, do not form supported lipid bilayers, we suggest that the presence of the egg PC vesicles/supported bilayer in mixtures with IM vesicles must in some way mediate IM vesicle rupture. Mixing the separate egg PC and IM vesicles through a process of

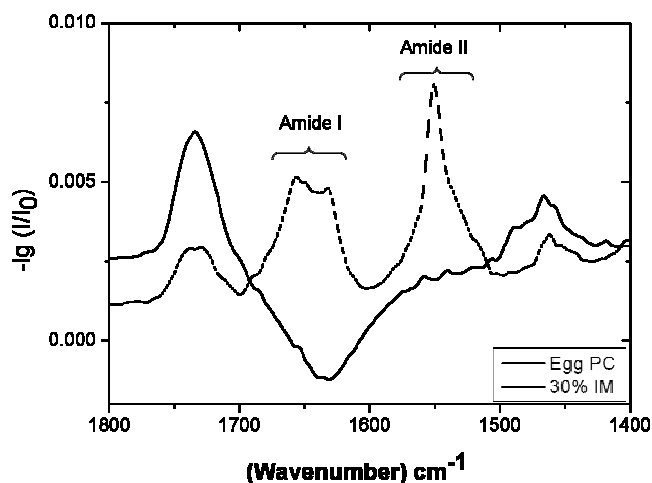


Fig. 6. ATR-FTIR spectrum of the amide I, II, and III regions for egg PC (black trace) and for SBLM formed with 30% IM (dashed black trace).

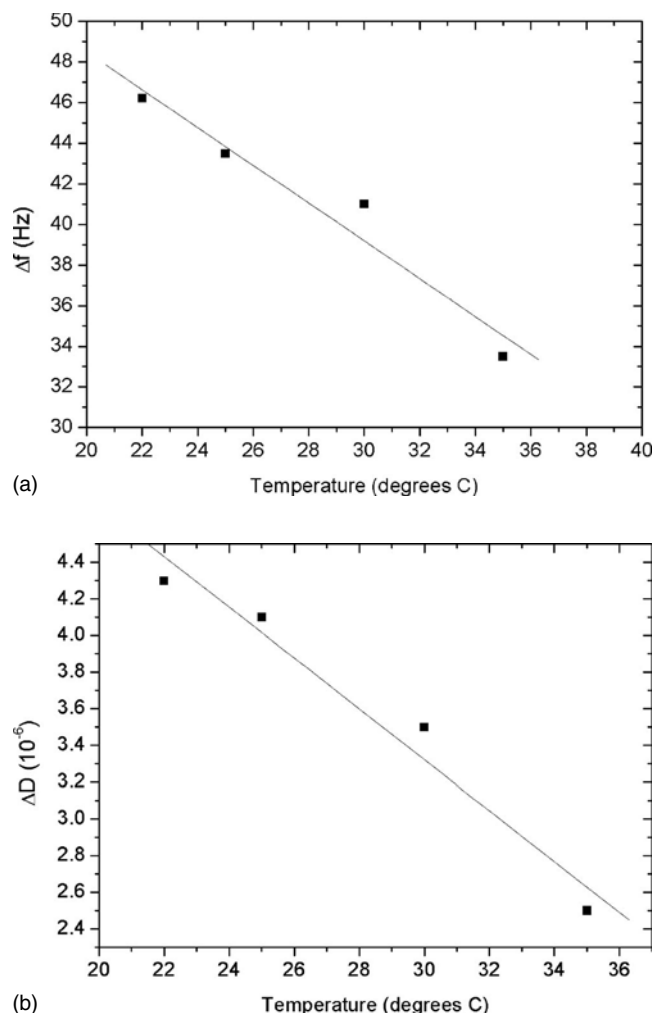


FIG. 7. Frequency ( $\Delta f$ ) and dissipation ( $\Delta D$ ) measured with QCM-D at increasing temperatures for a SBLM formed with 30% IM samples.

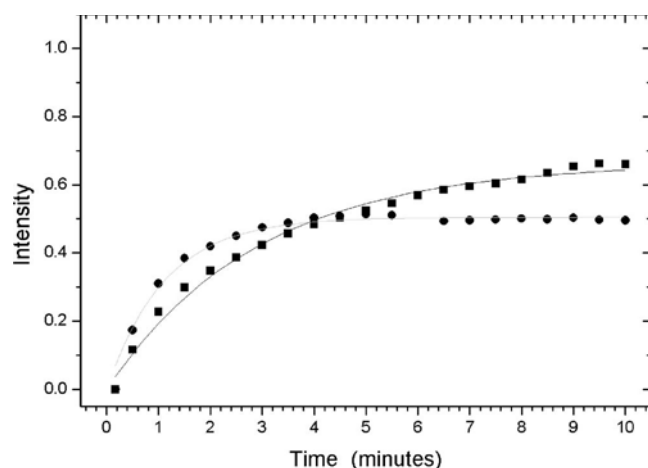


FIG. 8. FRAP experiments for membranes formed with 30% IM at 35 °C. The Texas Red fluorophore lipids from egg PC vesicles (black, square markers) and the NBD fluorophore lipids from IM vesicles (circular, gray markers).

TABLE I. The diffusion coefficients for Texas Red (egg PC) and for NBD (IM) in a 30% IM vesicle mixture measured at 22 and 35 °C.

Temperature (°C)	Diffusion coefficient egg PC (Texas Red)	Diffusion coefficient IM (NBD)
22°	0.35 $\mu\text{m s}^{-1}$	0.62 $\mu\text{m s}^{-1}$
35°	1.04 $\mu\text{m s}^{-1}$	3.73 $\mu\text{m s}^{-1}$

extrusion, three freeze-thaw cycles followed by a final extrusion process was also explored. However, membranes of better quality, i.e., yielding more planar bilayer characteristics, as determined by QCM-D and AFM, were produced through the tip sonication method presented here. QCM-D and FRAP data both show a clear improvement in the quality of SBLM formation for samples of 30% IM formed at 35 °C rather than 22 °C and, in particular, we find a pronounced increase in fluidity displayed by both fluorophores, i.e., those introduced from both the IM and the egg PC membranes. With this optimized system for incorporation of native bacterial membranes, we are now able to utilize the methodology to investigate more complex membrane processes. Current study is now underway into the *in vitro* biosynthesis of bacterial peptidoglycan utilizing the mixed membranes presented in this work. For such a system to be functional, certain enzymes are located in specific orientations. In a natural system, i.e., a whole, functional bacterium, enzymes are located on specific sides of the membrane, e.g., some on the cytoplasmic side of the membrane and some on the periplasmic side, in order for peptidoglycan biosynthesis to occur. Due to the method of isolation of the IM in this study, vesicles are produced both inside out and vice versa. This fact implies that the SBLMs formed here will have all the necessary enzymes required for peptidoglycan biosynthesis on both sides of the membrane. Preliminary data show that we can form peptidoglycan biosynthetically on SBLMs.<sup>30</sup>

## V. CONCLUSION

We have demonstrated here a simple method to incorporate substantial fractions of native *E. coli* inner membrane into solid-supported planar bilayer lipid membranes. This method represents a facile approach to incorporate numerous different protein types into a bilayer without requiring isolation and purification of each individual protein beforehand. In contrast to other approaches, we have also shown that with separate vesicle populations it is possible to generate a supported membrane containing both components. The vesicles which form a lipid bilayer readily do not prevent the other vesicles from forming a lipid bilayer, but appear to aid their incorporation. The bilayer membranes formed contain the membrane proteins from the IM fractions; these may account for features seen in AFM images. Finally, SBLMs formed, and maintained, at higher temperatures (35 °C) yielded higher quality bilayers with increased lipid diffusion rates.



## ACKNOWLEDGMENTS

This work was supported by the Biotechnology and Biological Sciences Research Council Grant No. BB/D00943X/1. The authors are grateful to Peter Henderson, Biochemistry, Leeds University for access to biochemistry facilities. The authors are also grateful to Andreas Erbe for valuable discussion. C. E. Dodd acknowledges support from the Engineering and Physical Sciences Research Council.

- <sup>1</sup>B. Alberts *et al.*, *Molecular Biology of the Cell*, 4th ed. (Garland Publishing, New York, 2000).
- <sup>2</sup>M. Gerstein and H. Hegyi, *FEMS Microbiol. Rev.* **22**, 277 (1998).
- <sup>3</sup>D. J. Muller, *Biophys. J.* **91**, 3133 (2006).
- <sup>4</sup>T. Rabilloud, *Nat. Biotechnol.* **21**, 508 (2003).
- <sup>5</sup>E. Wallin and G. von Heijne, *Protein Sci.* **7**, 1029 (1998).
- <sup>6</sup>H. Aquila, T. A. Link, and M. Klingenberg, *FEBS Lett.* **212**, 1 (1987).
- <sup>7</sup>G. McDermott *et al.*, *Nature (London)* **374**, 517 (2002).
- <sup>8</sup>D. Bramhill, *Annu. Rev. Cell Dev. Biol.* **13**, 395 (1997).
- <sup>9</sup>D. K. Miller *et al.*, *Nature (London)* **343**, 278 (1990).
- <sup>10</sup>G. L. Scheffer *et al.*, *Cancer Res.* **60**, 2589 (2000).
- <sup>11</sup>J. Hardy, *Trends Neurosci.* **20**, 154 (1997).
- <sup>12</sup>T. R. Jahn and S. E. Radford, *FEBS J.* **272**, 5962 (2005).
- <sup>13</sup>A. L. Hopkins and C. R. Groom, *Nat. Rev. Drug Discov.* **1**, 727 (2002).
- <sup>14</sup>H. M. McConnell, T. H. Watts, R. M. Weis, and A. A. Brian, *Proc. Natl. Acad. Sci. U.S.A.* **81**, 7564 (1984).
- <sup>15</sup>T. H. Watts, H. E. Gaub, and H. M. McConnell, *Nature (London)* **320**, 179 (1986).
- <sup>16</sup>N. Boden *et al.*, *Tetrahedron* **53**, 10939 (1997).
- <sup>17</sup>K. H. Sheikh, H. K. Christenson, R. J. Bushby, and S. D. Evans, *J. Phys. Chem. B* **111**, 379 (2007).
- <sup>18</sup>I. Reviakine and A. Brisson, *Langmuir* **16**, 1806 (2000).
- <sup>19</sup>L. J. C. Jeuken *et al.*, *J. Am. Chem. Soc.* **128**, 1711 (2006).
- <sup>20</sup>C. A. Keller and B. Kasemo, *Biophys. J.* **75**, 1397 (1998).
- <sup>21</sup>V. P. Zhdanov, K. Dimitrievski, and B. Kasemo, *Langmuir* **22**, 3477 (2006).
- <sup>22</sup>K. Tawa and K. Morigaki, *Biophys. J.* **89**, 2750 (2005).
- <sup>23</sup>B. R. J. Johnson, R. J. Bushby, J. Colyer, and S. D. Evans, *Biophys. J.* **90**, L21 (2006).
- <sup>24</sup>E. Reimhult, M. Zach, F. Hook, and B. Kasemo, *Langmuir* **22**, 3313 (2006).
- <sup>25</sup>D. Axelrod, D. E. Koppel, J. Schlessinger, E. Elson, and W. Webb, *Biophys. J.* **16**, 1055 (1976).
- <sup>26</sup>A. Erbe, R. J. Bushby, S. D. Evans, and L. J. C. Jeuken, *J. Phys. Chem. B* **111**, 3515 (2007).
- <sup>27</sup>*Structural Investigations of Oriented Membrane Assemblies by FTIR-ATR Spectroscopy*, edited by J. A. de Haseth, The Eleventh International Conference on Fourier Transform Spectroscopy (ICOFTS-11) (American Institute of Physics Press, New York, 1997), Vol. 430, p.729.
- <sup>28</sup>Z. Salamon, Y. Wang, J. L. Soulages, M. F. Brown, and G. Tollin, *Biophys. J.* **71**, 283 (1996).
- <sup>29</sup>Z. Salamon, J. T. Hazzard, and G. Tollin, *Proc. Natl. Acad. Sci. U.S.A.* **90**, 6420 (1993).
- <sup>30</sup>M. J. Spenceley *et al.*, *Angew. Chem.* **118**, 2165 (2006).
- <sup>31</sup>*Microbial Lipids*, edited by C. Ratledge and S. G. Wilkinson (Academic Press, Harcourt Brace Jovanovich, London, 1988, Vol. 1).
- <sup>32</sup>L. J. C. Jeuken *et al.*, *Langmuir* **21**, 1481 (2005).
- <sup>33</sup>A. Graneli, J. Rydstrom, B. Kasemo, and F. Hook, *Langmuir* **19**, 842 (2003).
- <sup>34</sup>L. Jeuken *et al.*, *J. Am. Chem. Soc.* **128**, 1711 (2006).
- <sup>35</sup>L. Jeuken *et al.*, *Sens. Actuators B* **124**, 501 (2007).
- <sup>36</sup>H. Schneider, J. J. Lemasters, M. Hochli, and C. R. Hackenbrock, *J. Biol. Chem.* **255**, 3748 (1980).
- <sup>37</sup>C. Elie-Caille, O. Fliniaux, J. Pantigny, J.-C. Maziere, and C. Bourdillon, *Langmuir* **21**, 4661 (2005).
- <sup>38</sup>R. Lovitt *et al.*, *Process Biochem.* **36**, 415 (2000).
- <sup>39</sup>P. K. Smith *et al.*, *Anal. Biochem.* **150**, 76 (1985).
- <sup>40</sup>M. Rodahl and B. Kasemo, *Rev. Sci. Instrum.* **67**, 3238 (1996).
- <sup>41</sup>D. M. Soumpasis, *Biophys. J.* **41**, 95 (1983).
- <sup>42</sup>K. J. Seu, L. R. Cambrea, R. M. Everly, and J. S. Hovis, *Biophys. J.* **91**, 3727 (2006).
- <sup>43</sup>K. C. Weng, J. Kanter, W. H. Robinson, and C. W. Frank, *Colloids Surf. B* **50**, 76 (2006).
- <sup>44</sup>L. Salomé, J.-L. Cazeils, A. Lopez, and J.-F. Tocann, *Eur. Biophys. J.* **27**, 391 (1998).
- <sup>45</sup>M. Weiss, *Traffic* **5**, 662 (2004).